Geophys. J. Int. (2002) **148,** 676–686

Effects of mantle flow law stress exponent on postglacial induced surface motion and gravity in Laurentia

Patrick Wu

Department of Geology & Geophysics, University of Calgary, Calgary, Alberta, Canada. E-mail: ppwu@ucalgary.ca

Accepted 2001 September 28. Received 2001 August; in original form 2000 September 15

SUMMARY

Recent studies show that power-law rheology with stress exponent $n = 3$ in the lower mantle or in a thin zone just beneath the lithosphere are consistent with the sea level observations in and around Laurentia. In this study, the stress exponent n is varied from 2 to 4, and for each value of n, a range of creep parameter A^* is searched to find the earth model that gives the best fit to the sea level observations in and around Laurentia. The effects of stress exponent on other geophysical observables—namely present day uplift rate, horizontal velocity, free-air gravity and the rate of change in gravity are also studied. The model used to calculate the postglacial readjustment of the Earth is a 3-D finite element model that includes realistic ice histories and eustatic water loads on stratified incompressible viscoelastic Maxwell flat-earths. Three types of earth rheology models are considered—the first one has nonlinear rheology throughout the mantle and the second has a nonlinear zone at the top of the mantle below the elastic lithosphere and a linear mantle. The third one has nonlinear rheology restricted to lie in the lower mantle. It is found that the models with nonlinear rheology in the lower mantle give better fits to the sea level data in and around Laurentia than the first two types. However, sea level data, when taken as a whole, cannot clearly discriminate between the stress exponents 2, 3 or 4. Present day uplift rate, horizontal velocity and rate of gravity change however may be useful in further discriminating mantle rheology.

Key words: gravity, horizontal velocity, mantle rheology, postglacial rebound, sea level, uplift rate.

1 INTRODUCTION

The dynamics of the Earth are strongly influenced by mantle rheology. For example, flow in the mantle becomes more localized as the value of the stress exponent in the flow law increases (e.g. Yuen & Schubert 1976). In general, the flow law is linear at low stress levels or small grain size. On the other hand, at high stress levels or large grain size, power-law dominates. However, the transition stress conditions between the different creep mechanisms are uncertain by an order of magnitude (Ranalli 1998), therefore microphysics is unable to tell definitively the value of the stress exponent in the mantle flow law.

Our approach is to infer mantle rheology from geophysical observations such as postglacial sea levels, present-day uplift rate, horizontal velocity and the rate of change in gravity around Laurentia. However, the calculation of these geophysical observable in a nonlinear medium is not simple. First, the conventional spectral method cannot be used to calculate Earth deformations (e.g. Peltier 1998) or sea levels (e.g. Mitrovica & Peltier 1991) because the principle of superposition does not apply when the problem is nonlinear. Second, analytical solutions do not exist for this problem. To make progress, simplifying assumptions were introduced in earlier work (Post & Griggs 1973; Brennen 1974; Crough 1977; Yokokura & Saito 1978; Nakada 1983). However, as pointed out by Wu (1992), some of these assumptions are invalid while others are too restrictive. Following Wu (1992) and Gasperini *et al.* (1992), the Finite Element (FE) method is used to calculate the Earth's response to surface ice/water loading since none of the simplifying assumptions has to be made and the solution is much more rigourous. Furthermore a number of commercial finite element packages have become available for such computation. However, two problems must be solved before commercial FE packages can be used—this is because commercial packages are generally designed for engineering purposes and the important effects of pre-stress advection (i.e. buoyancy) and self-gravitation are not included. The inclusion of these effects in the FE code is not straightforward. Wrinkler foundations can simulate the former—but the meaning of the stress field has to be reinterpreted. The inclusion of self-gravitation in a spherical FE model is more difficult (Giunchi & Spada 2000) and the problem has only been solved very recently (Wu, in preparation). However, the inclusion of self-gravitation and sphericity in the FE method is much more computational intensive if one wants to achieve high spatial resolution (<500 km). Fortunately, Wu & Johnston (1998) showed that relative displacements computed with the FE method on a 3-D

incompressible non-self-gravitating flat earth, do give excellent approximations to relative sea levels computed with the sea level equation in a spherical self-gravitating incompressible earth—provided that the sea level sites do not lie too far from the centre of rebound and the age of the sea level data is within the last 8 ka. Since the flat earth model is computationally more efficient, we will continue to use it for this study.

An added complication in the study of postglacial re-adjustment with nonlinear rheology is due to the dependence of the effective viscosity on stress (see eq. (3) below). The state of stress has two contributions: ambient tectonic stress (e.g. due to mantle convection) and load induced stress (e.g. from ice and water loads). Unfortunately, neither the tectonic stress nor the ice/water load history is well determined at the present so that the effective viscosity is not a predetermined quantity in the equation of motion. The problem may be less severe because the strain magnitude due to postglacial rebound is orders of magnitude smaller than that due to tectonics—thus there may be no interaction between rebound stress and tectonic stress (Karato 1998). This is the assumption taken in this paper and the advantage is that we no longer need to consider the influence of ambient stress. (Wu 2001, has investigated the effect of tectonic stress on postglacial readjustment in a uniform mantle with power-law rheology.) However, the coupling of ice/water load with Earth rheology means that one can no longer determine mantle rheology independent from the ice load history. (The water load history can be determined when both the ice history and Earth rheology are given.) To infer mantle rheology from geophysical observations, one needs to search iteratively for the rheology-ice model combination that gives the best fit to all geophysical observables related to postglacial readjustment by assuming in turn either the ice history or the rheological model as perfect inputs. The problem is that the result of such a search may depend on the starting rheology-ice model combination and the search may only lead to a local solution instead of the global solution.

Despite the difficulties mentioned above, a number of papers have worked towards the goal of understanding the influence of nonlinear rheology on postglacial readjustment. As reviewed by Wu (1998), results of earlier studies with simple loading history show that uniform mantles with nonlinear rheology cannot explain the sea level data immediately outside the Laurentian ice margin (e.g. near Boston). This is because the stress in a nonlinear uniform mantle induces a 'low viscosity channel' that terminates outside the load—as a consequence, the peripheral bulge in a nonlinear uniform mantle do not migrate but just collapse in place after deglaciation (Wu 1993, 1995). This behaviour is intermediate between that of deep flow, where the peripheral bulge migrate inwards as it collapses, and that of channel flow where the peripheral bulge migrates outwards. But in order to explain the observed sea level data immediately outside the Laurentian ice margin, the peripheral bulge must migrate inwards during its collapse, thus producing the observed land emergence followed by submergence seen in the sea level record within the 'Relative Sea level Transition Zone' (e.g. near Boston).

Combining microphysics, seismic anisotropy observations and postglacial rebound modelling with simple ice histories, Karato & Wu (1993) suggested that the top 300 km of the mantle may be nonlinear but the flow law becomes linear below that depth. Such an earth model has recently been shown by Wu (1999) to give better fit to the sea level data in and around Laurentia than the model with a linear 10^{21} Pa-s uniform mantle when realistic ice histories are used.

A surprising result from Wu (1999) is that, the model with a nonlinear lower mantle below a linear 10^{21} Pa-s upper mantle and 150 km thick elastic lithosphere, provided superior fits to the sea level data in and around Laurentia than the nonlinear channel model proposed by Karato & Wu (1993). This is contrary to the finding of Karato & Li (1992) and Li *et al.* (1996) who proposed that the lower mantle may be linear based on high temperature creep data of some relevant rock material. Thus the results of Wu (1999) calls into question the relevance of these data for creep in the lower mantle when the strain rate is much larger than the geological strain rate.

In the investigation of Wu (1999), the stress exponent in the nonlinear lower mantle is taken to be 3 only and the sensitivity of the sea level predictions to changes in the value of the creep parameter A^* has not been investigated. However, studies of the creep law in olivine polycrystals and materials with perovskite structure (e.g. Chopra & Paterson 1981; Wang *et al.* 1993) show that the stress exponent may be closer to 4, and for grain-size sensitive creep, the stress exponent is likely to be slightly less than 2 (Karato 1989). Thus, the main purpose of this paper is to investigate the effects of stress exponent on postglacial induced surface motion and gravity to see if the observed data can discriminate the value of the stress exponent $n = 2, 3$ or 4. The only linear rheology model considered is a uniform 10^{21} Pa-s mantle, this will be our reference model. Other linear rheology models will not be included because they have been studied in many other works.

Wu (1999) only considered sea level data in his study but recent investigations of the postglacial readjustment process include observations in uplift rates, horizontal velocities, changes in the geopotential field, the Earth's rotational motion and fault instability. Therefore it is desirable to have predictions for some of these other observable, as they may provide extra constraints on mantle rheology.

In summary, the purpose of the present paper is to: (1) study the effects of stress exponent n on the postglacial induced surface motion and gravity. (2) For each value of n, the creep parameter A^* is searched to find the value that best fits the sea level data around Laurentia. (3) To extend the results of Wu (1999) to include predictions of uplift rate, horizontal velocity, free air gravity anomaly and the rate of change of gravity in order to further constraint mantle rheology.

2 THE MODEL

All earth models considered here are isotropic, incompressible, viscoelastic flat-earths with power-law rheology and no self-gravitation. Wu & Johnston (1998) have demonstrated that the flat-earth approximation is adequate in describing land uplift due to loads even as large as the Laurentian ice sheet. Because compressibility mainly affects the amplitude of the sea level curves and cannot change land emergence to submergence or vice versa, incompressibility is assumed here to keep the problem simple. However, one must be cautioned that the effects of Earth sphericity and compressibility on horizontal motion are not well understood at the present, thus further studies are needed to verify our conclusions about horizontal motion.

It is further assumed in this study that the rebound process sees the steady state creep and that there is little or no interaction between rebound stress and the ambient tectonic stress. The assumption of steady-state creep has been questioned by Karato (1998)—but the problem of transient creep and tectonic-rebound stress interaction has been addressed elsewhere (e.g. Wu 2001).

For a viscoelastic material, the deformation can be decomposed into the elastic response and the creep response. The elastic strain

Table 1. Elastic parameters of stratified earth models.

	Depth	Density (kg m^{-3})	Young's modulus (Pa)	Poisson ratio
Lithosphere	0–150 km	3475	1.92×10^{11}	0.5
Layer 1	150–420 km	3475	2.16×10^{11}	0.5
Layer 2	420–670 km	3616	3.25×10^{11}	0.5
Lower mantle	Below 670 km	3888	6.61×10^{11}	0.5

is related to the stress by Hooke's law while the steady state creep law is given by:

$$\dot{\varepsilon}_{ij}^{C} = A^{*}\sigma_{E}^{\prime n-1}\sigma_{ij}^{\prime} \tag{1}$$

Here A^* is the creep parameter, $\sigma_{ij}^{\prime}$ are the deviatoric stress components and $\sigma_{E}^{\prime}$ is the equivalent deviatoric stress with

$$\sigma_{E}^{\prime} = \sqrt{\frac{1}{2}\sigma_{ij}^{\prime}\sigma_{ij}^{\prime}} \tag{2}$$

For linear rheology, n equals 1. For nonlinear rheology, n is taken to lie between 2 and 4 in this study (Chopra & Paterson 1981; Wang *et al.* 1993; Karato 1989; Goetze & Kohlstedt 1973). The range of the creep parameter A^* used is consistent with that deduced from microphysics if reasonable values of activation enthalpy and temperature are used (Karato 1989). For later discussion and comparison of results with other papers, it is useful to define the effective viscosity as:

$$\eta_{\text{eff}} = \frac{1}{3A^{*}\sigma_{\text{E}}^{\prime(n-1)}} \tag{3}$$

which says that large stress level (e.g. from the load) will result in low effective viscosity.

The earth models considered here all contain a 150 km thick elastic lithosphere overlying a stratified viscoelastic mantle and an inviscid fluid core. Since the effect of lithospheric thickness is not significant enough to change land emergence to submergence or vice versa, and the thickness under North America is poorly constrained, an intermediate value between the traditional value of 100 km (Walcott 1970) and the 200 km proposed by Peltier (1984) is adopted. The elastic parameters of the earth models are listed in Table 1.

Three types of rheology models are investigated. In the models of Table 2, both the upper mantle and lower mantle have the same parameters. The letter U in the name of the model indicates that the rheology is uniform and the number following it gives the stress exponent. Model U1 is the reference model that has a linear uniform viscosity of 10^{21} Pa-s in the mantle. The model proposed by Karato & Wu (1993) is listed in Table 3. Here the name NLZ denotes 'nonlinear zone' below the lithosphere but above 300 km depth. Wu (1999) has confirmed that as the thickness of the nonlinear zone increases, so does the misfit to the sea level data (Chi-square statistics). In Table 4, the names of these models start with NLLM meaning that they all have a linear upper mantle overlying a Non-Linear Lower Mantle. Again, the number in the name is the stress exponent in the nonlinear part of the mantle. A range of values for the creep parameter A^* will be searched to find the models that best-fit the sea level data around Laurentia.

Table 2. Rheologic structure of the uniform models.

	Model			
Name	U1	U2	U3	U4
Lithospheric thickness (km)	150	150	150	150
Stress exponent n in mantle	1	2	3	4
A^* in the mantle (Pa^{-n} s^{-1})	3.33×10^{-22}	Variable	Variable	Variable
χ^2	5.4		See Fig. 1	

Table 3. Nonlinear zone below the lithosphere but above 300 km depth.

	Model		
Name	NLZ2	NLZ3	NLZ4
Lithospheric thickness (km)	150	150	150
n in nonlinear zone	2	3	4
A^* in nonlinear zone (Pa^{-n} s^{-1})	Variable	Variable	Variable
Thickness of nonlinear zone (km)	150	150	150
n in the mantle (below nonlinear zone)	1	1	1
A^* in the mantle (Pa^{-1} s^{-1})	3.33×10^{-22}	3.33×10^{-22}	3.33×10^{-22}

The 3-D Finite Element Model used to calculate the deformation of the earth due to glacial loading and unloading is composed of 10 layers with each layer consisting of 1088 three-dimensional 8-node elements covering a total area of 240,000 by 240,000 km. However, only results in the central region are intended to be useful. The grid there is the densest and includes 14×12 elements, each with horizontal dimensions of 340×323 km—which is close to the spatial resolution of the ice model. The details of the Finite Element model can be found in Wu & Johnston (1998), who also showed that the relative displacement curves computed with the FE method on a 3-D flat-earth give excellent approximation to the relative sea level curves computed with the consistent sea level equation (Mitrovica & Peltier 1991) for a spherical self-gravitating earth.

The ice model is adapted from the ICE3G model of Tushingham & Peltier (1991). It consists of the Laurentian, Cordillera, Innuition and Greenland ice-sheets. The ICE3G model is used here because it provides reasonable fit to a large number of relative sea level observations even when nonlinear rheology is used (Wu 1999). Obviously, many other ice models need to be examined in order to understand how the ice load may effect our search for mantle rheology (see eq. 3). But due to the limited scope of this paper, only the ICE3G model will be used here.

Several saw-tooth glacial cycles that have slow build-up time of 90 ka but rapid deglacial time of 10 ka is assumed to precede the deglaciation history given by ICE3G. Increasing the number of glacial cycles do not significantly affect our results. Eustatic ocean loading due to melting of all the ice sheets in ICE3G is also included.

Table 4. Linear upper mantle with nonlinear lower mantle.

	Model		
Name	NLLM2	NLLM3	NLLM4
Lithospheric thickness (km)	150	150	150
n in upper mantle	1	1	1
A^* in upper mantle (Pa^{-1} s^{-1})	3.33×10^{-22}	3.33×10^{-22}	3.33×10^{-22}
n in lower mantle (below 670 km)	2	3	4
A* in lower mantle (Pa^{-n} s^{-1})	Variable	Variable	Variable

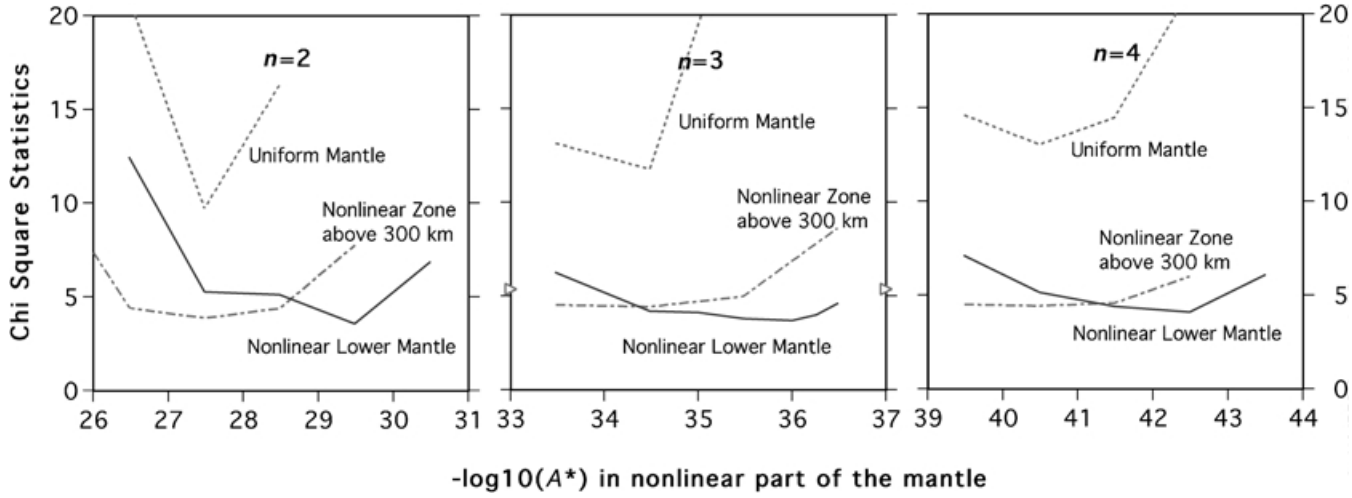

Figure 1. Chi-Square statistics as a function of creep parameter A^* for stress exponent $n = 2$, 3 and 4. Dotted lines are for models with nonlinear uniform mantle (Table 2), chain dashed lines are for the NLZ models (Table 3) and solid lines are for NLLM models (Table 4).

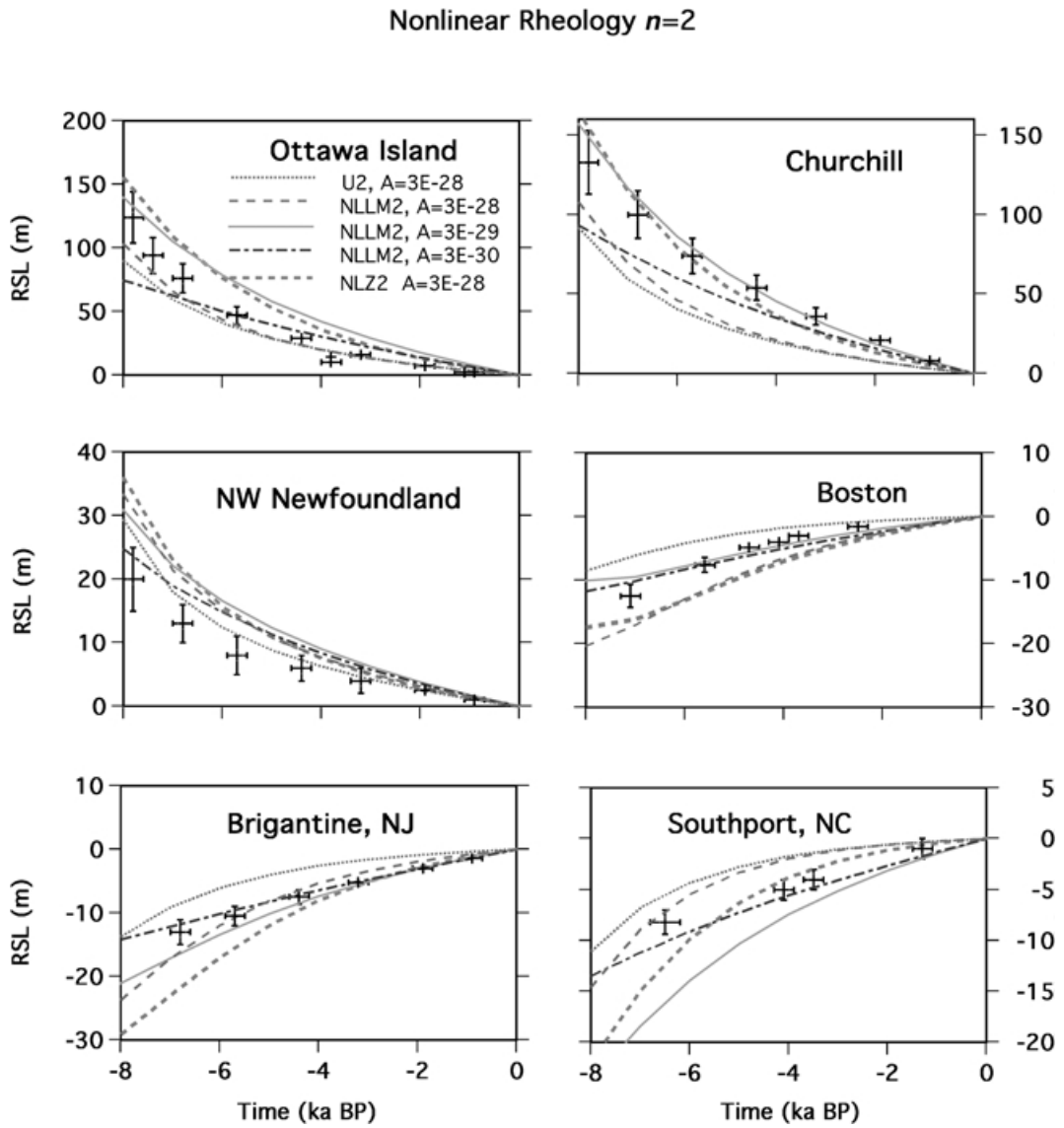

Figure 2. Comparing the predicted and observed sea level data at six sites in eastern Canada and along the US east coast for model U2, NLZ2 and three selected NLLM2 models (Tables 2, 3 and 4).

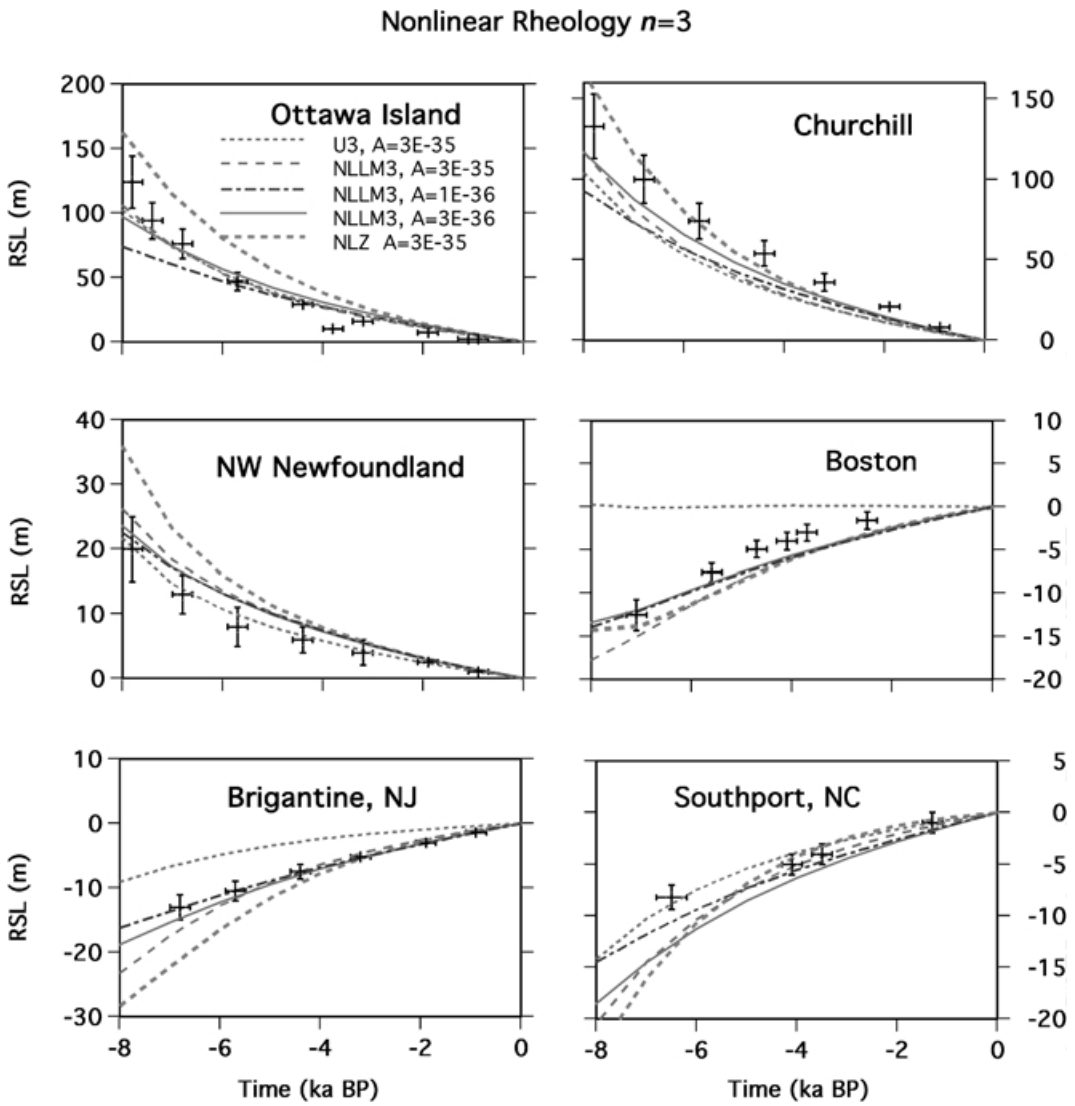

Figure 3. Similar to Fig. 2 except for models U3, NLZ3 and three selected NLLM3 models.

3 RESULTS

3.1 Relative sea levels

In this subsection, the observed sea level data for 27 sites with lengthy records (13 are found inside the former ice margin while 14 are found outside) are compared to the relative displacement curves predicted by different earth models of Tables 2–4. To quantify the comparison, χ^2 (Chi-square) statistics are computed for each model. Here,

$$\chi^2 = \frac{1}{M}\sum_{n=1}^{M}\left(\frac{\zeta_{\text{observed}} - \zeta_{\text{predicted}}}{s}\right)^2 \tag{4}$$

where ζ_{observed}, $\zeta_{\text{predicted}}$, s and M are the observed sea levels, the predicted sea levels, the standard deviation of the error in height and the number of observations respectively. In this study, a total of 144 observations from the 27 sites are considered.

Fig. 1 summarizes the χ^2 statistics of the different rheological models given in Tables 2, 3 & 4. The negative of the logarithm of A^* is plotted along the horizontal axis, so that for a fixed equivalent stress level (see eq. 3), effective viscosity increases to the right. (Note that with A^* plotted this way, the value of $A^* = 3 \times 10^{-30}$ Pa^{-2} s^{-1} would lie between the 29 and 30 tick marks.) The triangles along the vertical axis indicate the χ^2 value for the reference model U1 that has 10^{21} Pa-s uniform viscosity throughout the mantle. This figure shows that earth models with uniform nonlinear rheology throughout the mantle (the U models) give much higher χ^2 values than those with nonlinear rheology restricted to the lower mantle (NLLM models) or to the thin zone just below the lithosphere (NLZ models). The best fitting models for n = 2, 3 and 4 have values of A* equal to 3×10^{-30} Pa^{-2} s^{-1}, 1×10^{-36} Pa^{-3} s^{-1} and 3×10^{-43} Pa^{-4} s^{-1} respectively in the lower mantle. For the NLZ models, the best fitting models for $n = 2$, 3 and 4 have values of A* equal to 3×10^{-28} Pa^{-2} s^{-1}, 3×10^{-35} Pa^{-3} s^{-1} and 3×10^{-41} Pa^{-4} s^{-1} respectively in the nonlinear zones at the top of the mantle. These NLZ models have slightly higher Chi-square statistics than the NLLM models, but the difference are not significant. Fig. 1 also shows that the chi-square statistics, when all the sea level data are considered together, cannot distinguish between the three values of stress exponent considered, but as we will see below, individual sea level curves do reveal the difference.

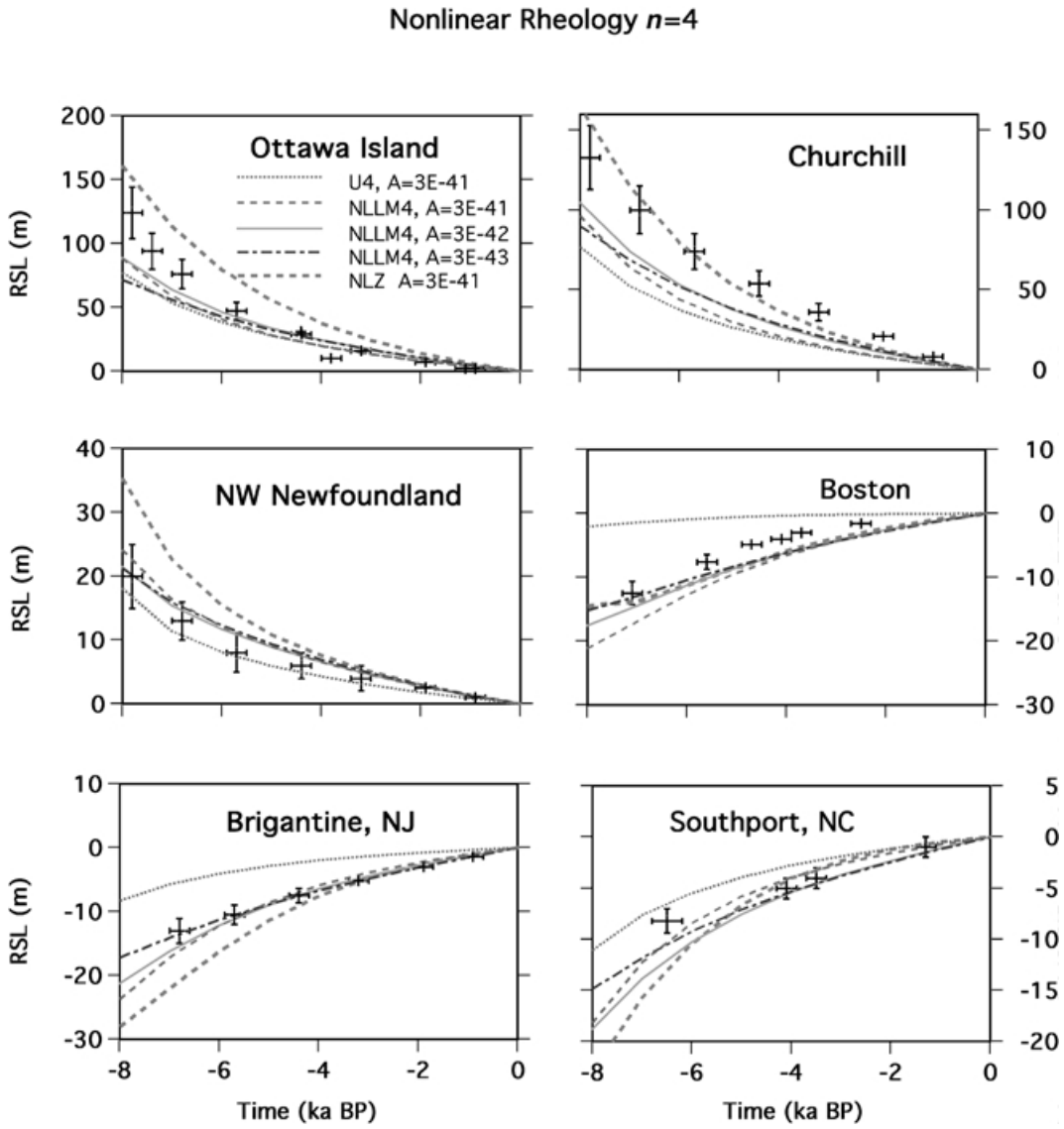

Figure 4. Similar to Fig. 2 except for models U4, NLZ4 and three selected NLLM4 models.

In Figs 2–4 visual comparisons between the data and the predictions of selected earth models at six representative sites are shown. For the NLZ models, only the one with the best chi-square statistics is included because varying the creep parameter, A^*, by one order of magnitude from the best value does not significantly change the fit to the sea level data. For sites immediately outside the ice margin (e.g. Boston and Brigantine), the best fitting nonlinear uniform mantles (i.e. U3, U4 & U2) still grossly underestimate the amplitude of submergence—in fact, even the best fitting U3 model predicts land emergence instead of submergence around Boston. As pointed out in Wu (1999), the reason of this is that nonlinear rheology in the upper mantle results in a stress induced low viscosity channel that terminates just outside the ice margin near Boston. For sites near the centre of rebound (e.g. Ottawa Island and Churchill), the nonlinear uniform models also under-predicts the height of the 8 ka BP beach. This is because the rebound rate was much higher near the end of deglaciation when the remaining load resulted in high stress and thus small effective viscosity just underneath the lithosphere (see eq. 3). To remedy this misfit in data near the centre of rebound, one may increase the local ice thickness. However, Wu (1999) showed that scaling the local ice thickness does give better fit to the data within the ice margin, however, misfits outside the ice margin do not improve. Thus, nonlinear uniform mantle cannot explain all the sea level data in and around Laurentia simultaneously. As shown in Wu (2001), an ambient tectonic stress level of 10 MPa is required to mitigate the misfit to the sea level data. However, even in that case, the χ^2 statistics are still worse than that for the reference model U1.

A much better fit to the sea level data is obtained for the NLLM and NLZ models, especially for sites outside the ice margin (e.g. Boston and Brigantine)—although the NLLM models do give slightly better fit to the data. Figs 2–4 also show that fine-tuning of the local ice thickness is required for sites within the ice margin. Finally, visual inspection of Figs 2–4 confirm that when all the sea level data are taken together, they give no preference to any of the stress exponents $n = 2$, 3 or 4.

3.2 Present-day velocities

From the preceding subsection, we saw that sea level data show no preference to any of the values of stress exponents considered.

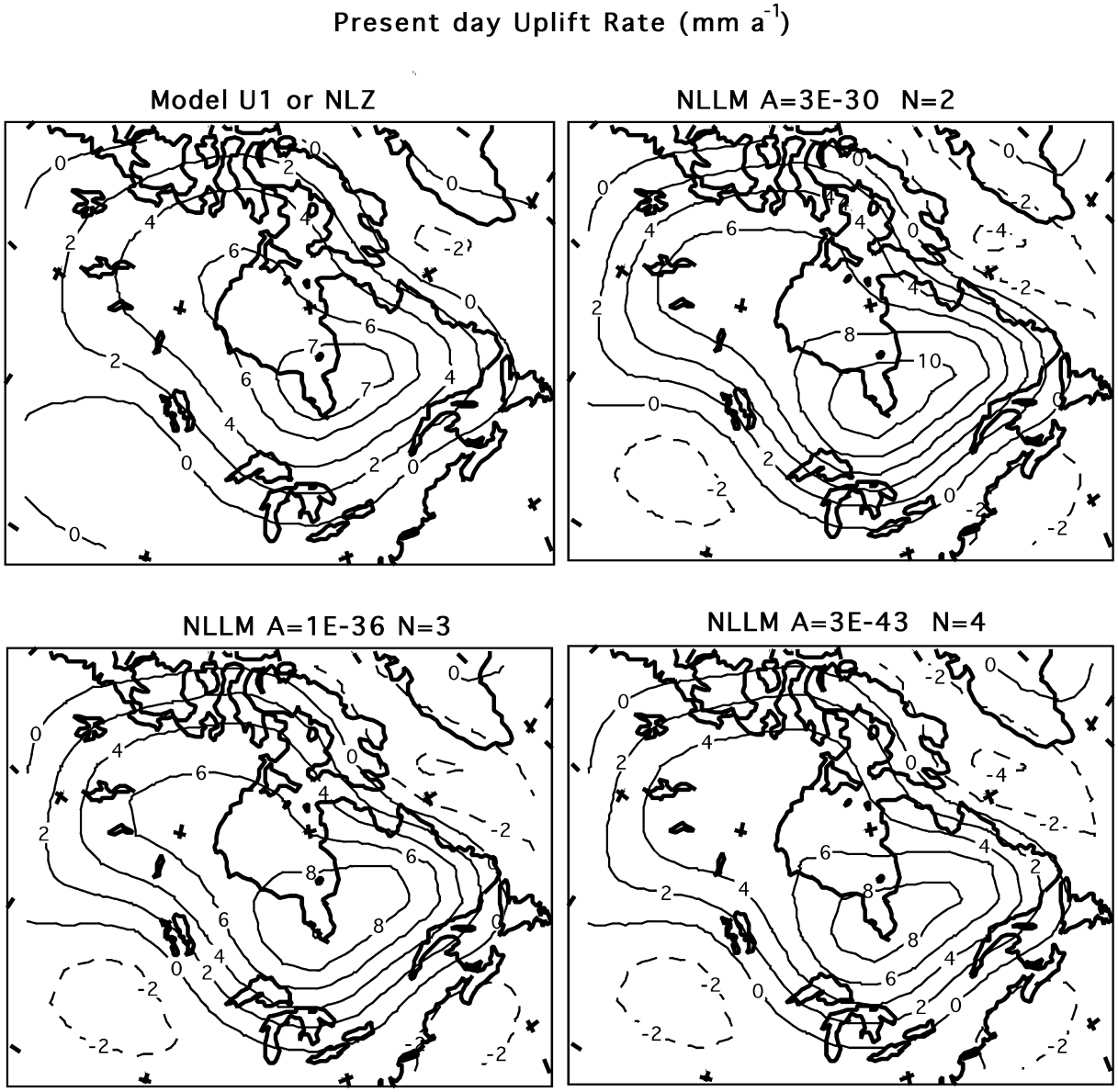

Figure 5. Present day uplift rate predicted by the four representative earth models (see text). Contours in mm a^{-1}. Solid contours for positive values, dashed contours for negative values.

However, due to recent advances in space-geodetic techniques such as GPS, VLBI, SLR and satellite altimetry, there are other geophysical observables related to the postglacial readjustment process which may provide further discrimination among the stress exponents. The ones that will be investigated in this subsection are the present-day land uplift rate and horizontal velocity in Eastern Canada—but as we shall see below, the motion within the ice margin are especially important. Unfortunately the GPS data there is quite sparse and at present not good enough to give a good constraint on mantle rheology. With the implementation of programs such as Canadian Base Network by the Geodetic Survey of Canada, this situation is now changing rapidly. It is hoped that in the near future, with denser and more accurate measurements, the observed horizontal motion can help to discrimination the stress exponents.

In view of the large number of earth models considered, we shall present here and in the next subsection only those models that give the best χ^2 statistics to the sea level data for each stress exponent. They are model NLLM2 with $A^* = 3 \times 10^{-30}$ Pa^{-2} s^{-1}, model NLLM3 with $A^* = 10^{-36}$ Pa^{-3} s^{-1}, model NLLM4 with $A^* = 3 \times 10^{-43}$ Pa^{-4} s^{-1} and model NLZ3. It should be noted that contour maps of the land uplift rate, horizontal velocity and gravity predicted by the best fitting NLZ2, NLZ3 or NLZ4 models are visually indistinguishable from each other and the reference model U1 despite the large differences revealed in relative sea level curves (Figs 2–4). This is because it is easier to pick out the long wavelength differences in contour maps than short wavelength variations, which show up more clearly in relative sea level curves. But the long wavelengths are sensitive to structures deeper than 300 km where the NLZ models are indistinguishable from each other and the uniform model U1.

Fig. 5 shows the present-day uplift rate predicted by these earth models. The pattern of uplift for all of them looks similar since that is mainly determined by the ice deglaciation history. However their amplitudes are slightly different—model NLZ3 (also NLZ2,

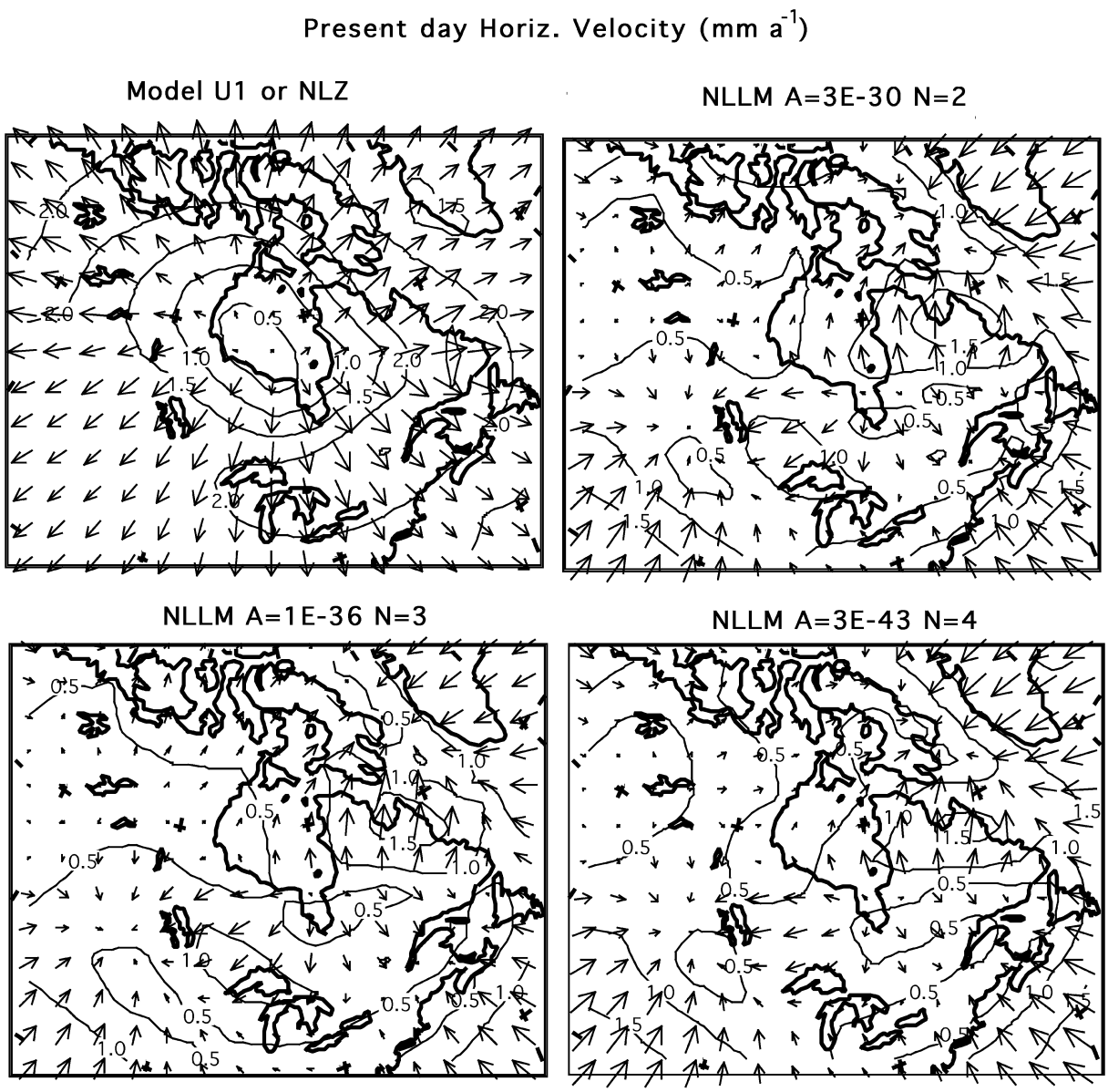

Figure 6. Present day horizontal velocity predicted by the four representative earth models (see text). Contours in mm a^{-1}. Solid contours for positive values, dashed contours for negative values.

NLZ4 and the reference model U1) has the smallest uplift rate while model NLLM2 has the largest value. Future refinement of geodetic techniques may be able to resolve these differences and help to constrain the stress exponent.

Fig. 6 shows the present-day horizontal velocities of these models. The arrows give the direction of the velocity vector and their lengths are proportional to its magnitude, which is also contour-plotted on the same diagram. While the NLZ or reference model U1 predicts that the motion is directed outwards from Hudson Bay, the pattern of horizontal motion in the NLLM models is completely different. Outside the ice margin, the motion is directed towards Hudson Bay just like that for a linear mantle that has very high viscosity in the lower mantle (channel flow). However, within the ice margin, the pattern is quite complex—motion is directed outwards from at least two centres, one in central Quebec and the other around Lake Athabasca in northern Saskatchewan. This is unlike the linear mantle that has high viscosity in the lower mantle, which predicts motion towards Hudson Bay even within the ice margin. Although the VLBI data in Eastern Canada and United States is sparse, the overall pattern tends to find more support from the NLLM models than from the deep flow models (U1 or NLZ models) or channel flow models. According to NASA Goddard Space Flight Center's VLBI Earth orientation series number er1122, (NASA 1999, prepared by Danial MacMillan and Chopo Ma), the horizontal motion outside the ice margin e.g. at NL_VLBA (North Liberty, Indiana), NLAO_140 (National Radio Astronomy Observatory, Green Bank, West Virginia) and MARPOINT (Maryland Point) are directed more-or-less towards the centre of rebound. In contrast, motion inside the ice margin e.g. at ALGOPARK (Algonquin Park, Ontario) is directed away from Hudson Bay but the magnitude there is small. Qualitatively, the relative motion between ALGOPARK and the other sites are consistent with the predictions from the NLLM models.

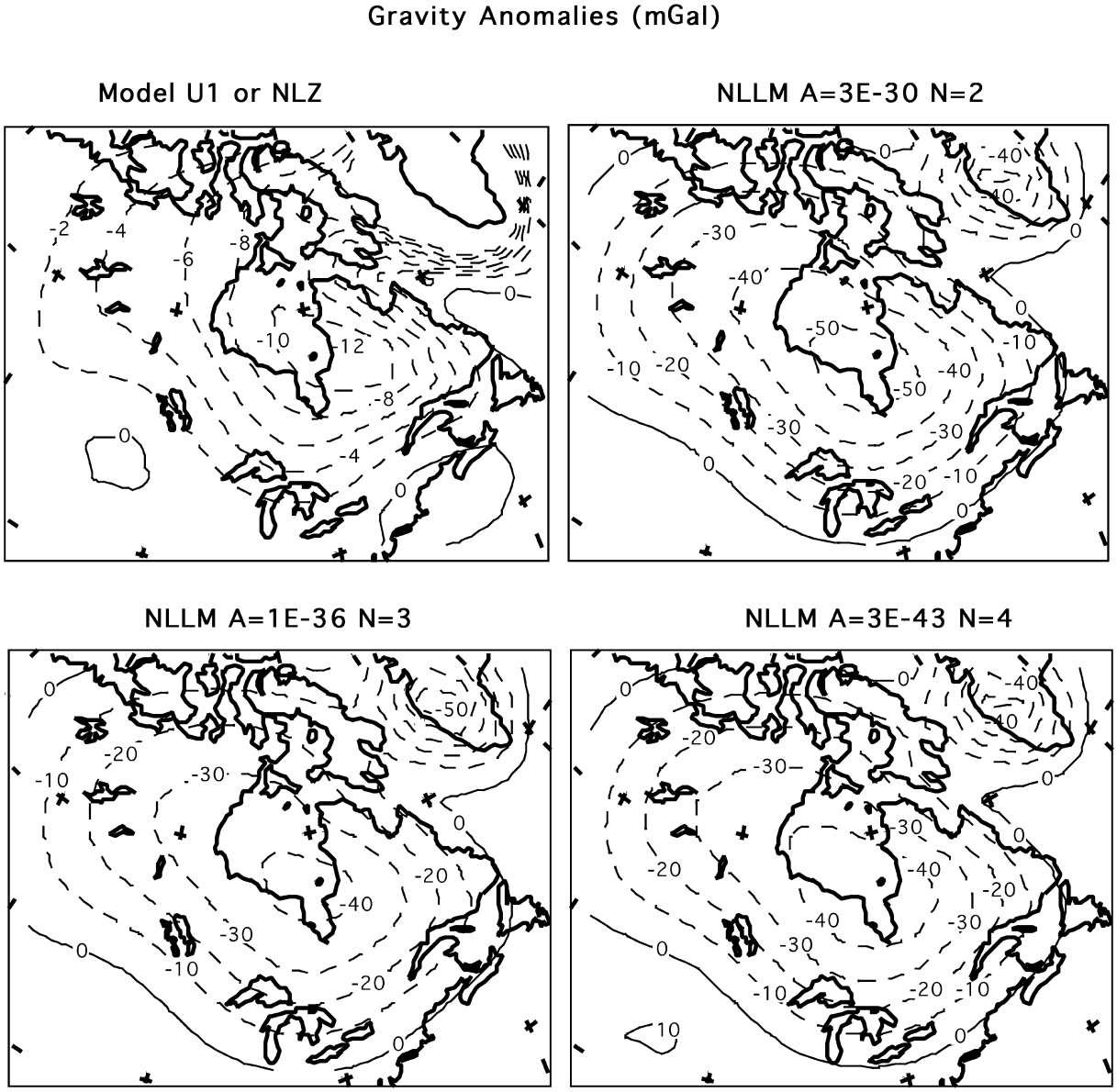

Figure 7. Present day free-air gravity anomaly predicted by the four representative earth models (see text). Contours in mGal. Solid contours for positive values, dashed contours for negative values.

However, quantitative comparison between the predicted and observed direction and magnitude of horizontal motion (e.g. Argus *et al.* 1999) are needed before any definitive conclusion can be drawn. Such comparison is not useful here because compressibility and sphericity have been neglected in our calculation. The magnitude and direction of horizontal motion are expected to be modified slightly when compressibility and sphericity are introduced. Also, viscosity stratification, lateral heterogeneity and ice history may also influence horizontal motion, thus the above results need to be confirmed with more refined modelling.

In short, Fig. 6 demonstrates that observations in horizontal velocity are potentially useful in discriminating between a mantle with deep flow (including the NLZ models), a linear mantle with high viscosity in the lower mantle (channel flow) and models with nonlinear lower mantle. However, all the NLLM models with different stress exponents give similar pattern and magnitude for the horizontal motion. Thus, in order to discriminate the stress exponents, the direction and magnitude of horizontal motion has to be determined with very high accuracies.

3.3 Gravity anomalies and the rate of change of gravity

In this subsection, we discuss present-day free air gravity anomalies and the rate of change of gravity for the four earth models in the last subsection. The gravity anomaly is derived from the current amount of uplift remaining by assuming a gravity-displacement ratio of 0.20 mGal m^{-1} (Wahr *et al.* 1995). Fig. 7 shows that the shape of the free air gravity anomalies for these earth models are similar but their magnitudes are different. Of these, model NLLM2 with $A^* = 3 \times 10^{-30}$ Pa^{-2} s^{-1} is able to predict -40 to -50 mGal over Hudson Bay which is close to the observed value of -30 to -47 mGal. Models NLLM4 with $A^* = 3 \times 10^{-43}$ Pa^{-4} s^{-1} and model NLLM3 with $A^* = 10^{-36}$ Pa^{-3} s^{-1} predict about -40 and -35 mGal respectively. The last prediction is slightly smaller than

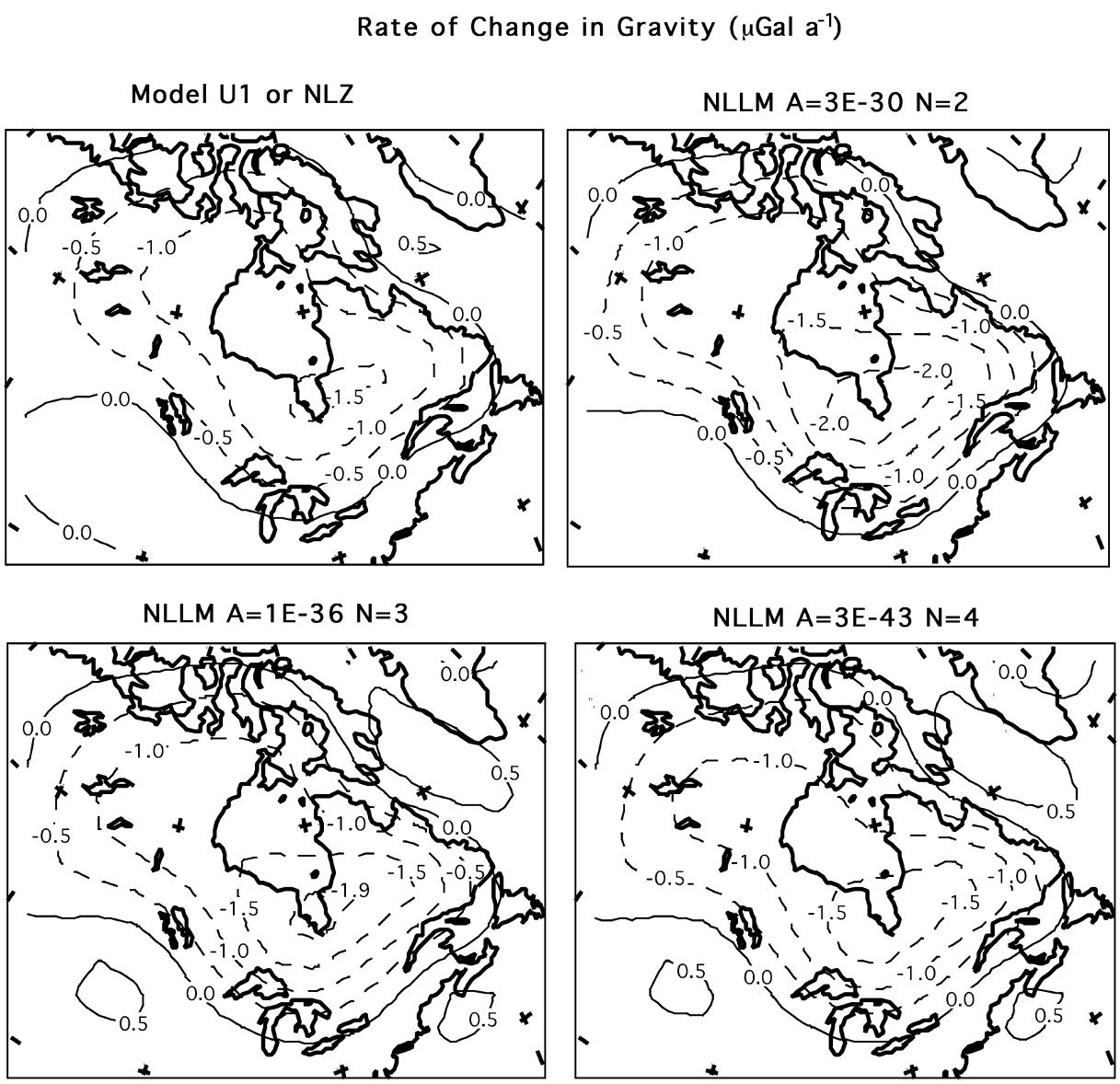

Figure 8. Present day rate of change in gravity predicted by the four representative earth models (see text). Contours in μGal a^{-1}. Solid contours for positive values, dashed contours for negative values.

the observed value. The U1 or NLZ models only predict -8 to -12 mGal over Hudson Bay—this is considerably less than the observed value. However, the observed magnitude (around -30 to -47 mGal) may have contributions from both postglacial rebound and dynamic topography induced by large scale mantle convection (Peltier *et al.* 1992) which can account for about -25 mGal of the observed anomaly. If Peltier *et al.* (1992) are correct, then the observed free air gravity favours the U1 or NLZ models more than the models with nonlinear uniform mantle.

Finally, the current rate of change of gravity can be obtained by multiplying the uplift rate by -0.20 mGal m^{-1} (Wahr *et al.* 1995) and the result is plotted in Fig. 8. Inspection of Fig. 8 shows that the peak rate of change in gravity is around the south tip of Hudson Bay which has value of about -1.5 μGal a^{-1} for the U1, NLZ and NLLM4 (with $A^* = 3 \times 10^{-43}$ Pa^{-4} s^{-1}) models. For model NLLM3 with $A^* = 10^{-36}$ Pa^{-3} s^{-1} and NLLM2 with $A^* = 3 \times 10^{-30}$ Pa^{-2} s^{-1}, the predicted values are about -1.9 and -2.1 μGal a^{-1} respectively. Since repeated absolute gravity measurements have been made in Churchill by the Geological Survey of Canada with the JILA-2 apparatus since about 1987 (Tushingham *et al.* 1991), it is useful to give the predicted values there. The values for the models NLZ (or U1), NLLM2, NLLM3 and NLLM4 at Churchill are: -1.2, -1.5, -1.4 and -1.3 μGal a^{-1} respectively. Thus, future measurements of the rate of change in gravity there may be useful in further discriminating mantle rheology and stress exponent.

4 CONCLUSIONS

In this paper we compared the predicted and observed sea level data around Laurentia for earth models with nonlinear rheology and different stress exponent. It is found that models with nonlinear rheology restricted to the lower mantle or to a thin zone just below the lithosphere give better fit to the sea level data than those with nonlinear rheology throughout the mantle or the reference model. These NLLM earth models can simultaneously explain the sea level data in and around Laurentia—although a slight increase in the local

ice thickness can further reduce the misfits to the observations there. However, sea level data when treated as a whole, cannot clearly discriminate between the stress exponents in the mantle flow law.

Uplift rate, horizontal velocity, free air gravity and the rate of change in gravity have also been calculated for four best fitting earth models. It is found that the horizontal velocity field is particularly useful in distinguishing between linear models with deep flow, channel flow or nonlinear rheology in the lower mantle. However, high precision measurements in horizontal velocities and better modelling are required to differentiate the stress exponents. Future models should include the effects of compressibility, self-gravitation and Earth sphericity. Furthermore, the effects of ice load histories, rheology stratification and lateral heterogeneity should all be investigated. With future improvement of geodetic techniques and more accurate observations in land uplift rate, free-air gravity anomaly and the rate of change in gravity, it may be possible to discriminate the stress exponents in the mantle flow law.

ACKNOWLEDGMENTS

The author would like to thank Editor Dr B.A. Buffett, and the two anonymous reviewers for their useful comments and to Chopo Ma for his useful help. This work is supported by a grant from NSERC (Canada). The finite element calculations were performed with the ABAQUS package from Hibbitt, Karlsson and Sorensen Inc.

REFERENCES

Argus, D.F., Peltier, W.R. & Watkins, M.M., 1999. Glacial isostatic adjustment observed using very long baseline interferometry and satellite laser ranging geodesy, *J. geophys. Res.,* **104,** 29 077–29 093.

Brennen, C., 1974. Isostatic recovery and the strain rate dependent viscosity of the earth's mantle, *J. geophys. Res.,* **79,** 3993–4001.

Chopra, P.N. & Paterson, M.S., 1981. The experimental deformation of dunite, *Tectonophysics,* **78,** 453–473.

Crough, S.T., 1977. Isostatic rebound and power-law flow in the asthenosphere, *Geophys. J. R. astr. Soc.,* **50,** 723–738.

Gasperini, P., Yuen, D.A. & Sabadini, R., 1992. Postglacial rebound with a non-Newtonian Upper Mantle and a Newtonian Lower Mantle Rheology, *Geophys. Res. Lett.,* **19,** 1711–1714.

Goetze, C. & Kohlstedt, D.L., 1973. Laboratory study of dislocation climb and diffusion in olivine, *J. geophys. Res.,* **78,** 5961–5971.

Giunchi, C. & Spada, G., 2000. Postglacial rebound in a non-Newtonian spherical earth, *Geophys. Res. Lett.,* **27,** 2065–2068.

Karato, S., 1989. Defects and plastic deformation in olivine, in *Rheology of Solids and of the Earth,* eds Karato, S. & Toriumi, M., pp. 176–208, Oxford University Press, Oxford.

Karato, S., 1998. Micro-physics of post glacial rebound, in *Dynamics of the Ice Age Earth: A Modern Perspective,* pp. 351–364, ed. Wu, P., Trans Tech Publ., Switzerland.

Karato, S. & Li, P., 1992. Diffusion Creep in Perovskite: implications for the rheology of the Lower Mantle, *Science,* **255,** 1238–1240.

Karato, S. & Wu, P., 1993. Rheology of the Upper Mantle: a synthesis, *Science,* **260,** 771–778.

Li, P., Karato, S. & Wang, Z., 1996. High-temperature creep of fine-grained polycrystalline CaTiO3, *Phys. Earth planet. Inter.,* **95,** 19–36.

Mitrovica, J.X. & Peltier, W.R., 1991. On postglacial geoid subsidence over the equatorial oceans, *J. geophys. Res.,* **96,** 20 053–20 071.

Nakada, M., 1983. Rheological structure of the earth's mantle derived from glacial rebound in Laurentide, *J. Phys. Earth,* **31,** 349–386.

NASA Goddard Space Flight Center VLBI Group, 1999. Data products available electronically at http://lupus.gsfc.nasa.gov/global.

Peltier, W.R., 1984. The thickness of the continental lithosphere, *J. geophys. Res.,* **89,** 11 303–11 316.

Peltier, W.R., 1998. A space geodetic target for mantle viscosity discrimination: Horizontal motions induced by glacial isostatic adjustment, *Geophys. Res. Lett.,* **25,** 543–546.

Peltier, W.R., Forte, A.M., Mitrovica, J.X. & Dziewonski, A.M., 1992. Earth's gravitational field: seismic tomography resolves the enigma of the Laurentian anomaly, *Geophys. Res. Lett.,* **19,** 1555–1558.

Post, R.L. & Griggs, D.T., 1973. The Earth's mantle: Evidence of non-Newtonian flow, *Science,* **181,** 1242–1244.

Ranalli, G., 1998. Inferences on mantle rheology from creep laws, in *Dynamics of the Ice Age Earth: A Modern Perspective,* pp. 323–340, ed. Wu, P., Trans Tech Publ., Switzerland.

Tushingham, A.M. & Peltier, W.R., 1991. Ice-3G: a new global model of late Pleistocene deglaciation based upon geophysical predictions of post-glacial relative sea-level change, *J. geophys. Res.,* **96,** 4497–4523.

Tushingham, A.M., Lambert, A., Liard, J.O. & Peltier, W.R., 1991. Secular gravity changes: measurements and predictions for selected Canadian sites, *Can. J. Earth Sci.,* **28,** 557–560.

Wahr, J., Han, D. & Trupin, A., 1995. Predictions of vertical uplift caused by changing polar ice volumes on a viscoelastic earth, *Geophys. Res. Lett.,* **22,** 977–980.

Walcott, R.I., 1970. Isostatic response to loading of the crust in Canada, *Can. J. Earth Sci.,* **7,** 716–727.

Wang, Z., Karato, S. & Fujino, K., 1993. High temperature creep of single crystal strontium titanate (SrTiO3): a contribution to creep systematics in perovskites. *Phys. Earth planet. Int.,* **79,** 299–312.

Wu, P., 1992. Deformation of an incompressible viscoelastic flat earth with power law creep: a finite element approach, *Geophys. J. Int.,* **108,** 136–142.

Wu, P., 1993. Post-glacial Rebound in a Power-law medium with Axial symmetry and the existence of the Transition zone in Relative Sea Level data, *Geophys. J. Int.,* **114,** 417–432.

Wu, P., 1995. Can observations of postglacial rebound tell whether the rheology of the mantle is linear or nonlinear?, *Geophys. Res. Lett.,* **22,** 1645–1648.

Wu, P., 1998. Postglacial rebound modelling with power law rheology, in *Dynamics of the Ice Age Earth: A Modern Perspective,* pp. 365–382, ed. Wu, P., Trans Tech Publ., Switzerland.

Wu, P., 1999. Modelling postglacial sea levels with power-law rheology and a realistic ice model in the absence of ambient tectonic stress, *Geophys. J. Int.,* **139,** 691–702.

Wu, P., 2001. Postglacial induced surface motion and gravity in Laurentia for uniform mantle with power-law rheology and ambient tectonic stress, *Earth planet. Sci. Lett.,* **186,** 427–435.

Wu, P. & Johnston, P., 1998. Validity of using Flat-Earth Finite Element Models in the study of postglacial rebound, in *Dynamics of the Ice Age Earth: A Modern Perspective,* pp. 191–202, ed. Wu, P., Trans Tech Publ., Switzerland.

Yuen, D.A. & Schubert, G., 1976. Mantle plumes: a boundary layer approach for Newtonian and Non-Newtonian temperature-dependent rheologies, *J. geophys. Res.,* **81,** 2499–2510.

Yokokura, T. & Saito, M., 1978. Viscosity of the upper mantle as non-Newtonian fluid, *J. Phys. Earth,* **26,** 147–166.